Fuel 320 (2022) 123964

Contents lists available at ScienceDirect

Fuel

journal homepage: www.elsevier.com/locate/fuel

An innovative high energy efficiency–based process enhancement of hydrogen liquefaction: Energy, exergy, and economic perspectives

Hyunhee Lee [a], Junaid Haider [a,*], Muhammad Abdul Qyyum [b], Changgwon Choe [a], Hankwon Lim [a,c,*]

[a] School of Energy and Chemical Engineering, UNIST, Ulsan, Republic of Korea
[b] Department of Petroleum & Chemical Engineering, Sultan Qaboos University, Muscat, Oman
[c] Department of Energy Engineering, UNIST, Ulsan, Republic of Korea

ARTICLE INFO

Keywords:
Hydrogen liquefaction
HFO based mixed refrigerants
Process enhancement
Specific energy consumption
Exergy efficiency

ABSTRACT

Hydrogen liquefaction can be one of the effective and viable solutions to enhance its energy contents for storage and transportation purposes. However, liquefaction of H_2 is highly energy intensive where precooling is the most significant energy consumption section (~50% of overall process) due to huge reduction in temperature (25 to −159.4 °C). In this context, in proposed study the precooling cycle is split into two cycles for reducing the energy consumption, 1) Hydrofluoroolefin–based mixed refrigerant stream which reduces the H_2 temperature to −30 °C and 2) Mixed refrigerant stream which tends to reduce the H_2 temperature up to −159.4 °C. This is the first study which utilizes the four refrigeration cycles with unique selection of HFO–based mixed refrigerants in precooling section to reduce the gaseous H_2 temperature. Results of proposed study reveal that the specific energy consumption of proposed process was reduced by 55.2 % and 29.5%, as compared to base case–I (10.15 kWh/kgLH_2) and base case–II (6.45 kWh/kgLH_2), respectively. The exergy efficiency of the proposed process was increased by 67%. In addition, results of economic evaluation depicted that the total annualized cost of proposed process was obtained as \$1.89 × 10^6 /y where the CAPEX has share of ~ 71.7% in total cost of project. The estimated unit production cost was recorded as \$5.18/kg of LH_2 at the capacity of 1TPD. The simplicity and less energy consumption of proposed model built a basis for its development to commercial scale adoption.

1. Introduction

Over a long period, fossil fuel economy is the prime source of energy despite of excessive environmental hazards. Therefore, controlling the corresponding environmental pollution caused by greenhouse gas emissions (GHGs) is a real global challenge, among which CO_2 emission is dominant. To cope up with these issues, worldwide agencies are forcing the energy–sectors, causing emissions of GHGs, to meet the environmental standards. In this regard, companies are focusing to reduce the carbon emissions up to specified permissible limit. While on the other hand, the expected energy demands are rapidly soaring to highest level that results in excess use of fossil fuels and relevant emissions are rapidly increasing. Thus, the world has dual challenge first to fulfill the ever-increasing energy demand and second is to limit the emissions.

In this context, developing the hydrogen (H_2) economy has been regarded as the potential replacement of the conventional fossil–based energy systems and a long–last solution for the challenges of climate change. It can be produced from different sources such as steam reforming of methane, water electrolysis, and from biomass. Considering the renewable solar/wind energy as power source, water electrolysis is one of the sustainable ways to produce green–H_2 [1,2]. Researchers have made efforts to improvised the water electrolysis technique by analyzing the different reference electrodes to provide the stable operation [3,4].

However, it is important to mention that the H_2 is an energy carrier and its production is carried out similarly as electricity and thus, interconvertible. Thus, sustainable development of hydrogen supply chain can be a futuristic approaches that may play a central role in global energy mix. Inversely, H_2 carries less energy density per unit volume that is a major challenge in its long-distance transportation. However, like natural gas liquefaction (LNG), hydrogen liquefaction (LH_2) is one of the most appropriate solutions to transport H_2. The LH_2 contains 3–4 times higher energy density and its capacity increased by 6 times than its compressed gas state [5,6]. Researchers are in continuous

* Corresponding authors at: School of Energy and Chemical Engineering, UNIST, Ulsan, Republic of Korea.
E-mail addresses: haiderjunaid92@gmail.com (J. Haider), hklim@unist.ac.kr (H. Lim).

https://doi.org/10.1016/j.fuel.2022.123964
Received 14 December 2021; Received in revised form 24 February 2022; Accepted 21 March 2022
Available online 30 March 2022
0016-2361/© 2022 Elsevier Ltd. All rights reserved.

Nomenclature

GHGs	Greenhouse gas emissions
H_2	Hydrogen
NG	Natural gas
LNG	Natural gas liquefaction
LH_2	Hydrogen liquefaction
TPD	Tons per day
SEC	Specific energy consumption
Ortho-H_2	Ortho hydrogen
Para-H_2	Para hydrogen
MR	Mixed refrigerant
TDCC	Temperature difference composite curve
THCC	Temperature heat flow composite curve
HFO	HFO-1234yf
BP	Boiling point
ODP	Ozone depletion potential
GWP	Global warming potential
CH_4	Methane
C_2H_6	Ethane
C_3H_8	Propane
n-C_4H_{10}	n-butane
i-C_4H_{10}	Iso-butane
N_2	Nitrogen
He	Helium
P_c	Critical pressure
T_c	Critical temperature
PR	Peng Robinson
MITA	Minimum temperature approach
OPC	Ortho to Para–H_2 conversion
MFC	mixed fluid cascaded
GH_2	Gaseous hydrogen
CHX	Cryogenic heat exchanger
h	enthalpy
s	entropy
ex_{ph}	Physical exergy
ex_{ch}	Chemical exergy
x	Mole fraction
μ_{ex}	Exergy efficiency
CAPEX	Capital cost
OPEX	Operating Cost
i	Discount rate
n	Project time
C	Capacity
I	Chemical engineering plant cost index (CEPCI)
C_{EC}	Capital cost of equipment
C_R	Reference cost
C_{RF}	Capital recovery factor
C_{BM}	Bare module cost
UPC	Unit production cost
AC	Annualized cost
COP	Coefficient of performance
FOM	Figure of merit

struggle to provide an efficient way for H_2 storage and transportation where liquid state transportation has significant importance.

In this context, small–scale ($\leq$0.5 TPD) and large–scale ($\geq$5 TPD) liquefiers differ in technology, from cryogenic refrigerators to open-loop thermodynamic cycles. Small liquefiers use the reverse helium Brayton cycle, while large liquefiers are generally designed with a Claude cycle [7].

Large-scale liquefiers require the use of isotopic conversion reactors as the reaction is very slow and exothermic.

Besides isotopic conversion, the minimum specific liquefaction power is affected by supply pressure and temperature between 1 and 60 bar and 283–303 K, respectively [8]. Generally, H_2 is in saturated liquid state at ≤ -253 °C under atmospheric pressure and the cryogenic liquefaction process to bring gaseous H_2 into LH_2 state is highly energy intensive $\sim$ 10–12 kWh/kg of LH_2, as per current LH_2 status. While, minimum ideal specific energy consumption (SEC) of H_2 liquefaction process is reported as 2.7 kWh/kg of LH_2 (IDEALHY project report) [9,10]. Regardless of the capacity, the current SEC of LH_2 processes is around 73–77.5% more than ideally required which means that the current processes can be further enhanced, intensified, and optimized to reduce this enormous gap. Another important factor is nuclei spin orientation of H_2 molecule that results in two of its isomers, Ortho-H_2 and Para-H_2. As the temperature drops down, the slight conversion of Para-H_2 is increased to establish an equilibrium state. It is important to notify that the para state is more stable and conversion process is quite slow. Furthermore, ortho to para conversion is exothermic which tends to increase the 15% more work requirement of overall liquefaction process [8,11]. Therefore, catalytic cryogenic operations are required to enhance the reaction rate.

To cope up with these issues, researchers are in continuous try to develop such a process with high energy efficiency and less exergy destruction. In this context, Cardella et al. [7,12] proposed the LH_2 processes based on pressurized Claude cycle and H_2–Ne cycle. It was investigated that the energy consumption in both processes can be reduced up to 6 kWh/kg LH_2 upon increasing the capacity of plant from 5 to 100 tons/d. In a study by Krasae-in et al [13], mixed refrigerants (MRs) based pilot scale model was developed to reduce the overall SEC specifically, the energy of precooling cycle. It was observed that the energy of precooling cycle was reduced up to 63.8%. However, this process has not considered the Ortho to Para–H_2 conversion reaction systems and the subcooling section contains 10 components to reduce the temperature by –193 °C with the installation of 4 Joule–Brayton cascade loops which enhances the process complexity despite of its high process efficiency (54%) [14]. Similarly, Sadaghiani et al. [15] proposed a LH_2 model with the utilization of MRs. The results of their study indicated that the SEC of the proposed process was reduced to 7.646 kWh/kg LH_2 while exergy efficiency was increased to 32%. Sadaghiani and Mehrpooya [16] have extended their idea with the implementation of two cooling cycles and two reaction systems for Ortho isomer to Para–H_2 isomer conversion. Results of their study reflected that the SEC was reduced to 4.41 kWh/kg LH_2 with high exergy efficiency 55.47%. However, the complexity of their process is a major obstacle in commercialization due to number of cryogenic exchangers and other process equipment. In another study, Qyyum et al. [17] have proposed a MRs cascade loop for hydrogen liquefaction. It was observed that the energy efficiency of the process is increased largely when mixed refrigerants were used to liquefy hydrogen in a combination of 3 refrigeration loops named as precooling, cooling, and liquefaction. In their process, two reaction systems were considered right after first and second cryogenic exchangers to convert the ortho isomer into para–H_2, the resulting conversion was 95% in para state with 100% saturated liquid and overall SEC of 6.45 kWh/kg LH_2. Naquash et al. [18] proposed a simulation model with 4 refrigeration loops. Among which, first was CO_2–precooled cycle that shares the load of precooling cycle and results in total SEC as 7.63 kWh/kg LH_2 and exergy efficiency around 31%. The authors have introduced an additional reaction system in comparison to other available studies which tends to increase the contents of Para–H_2 up to 99%. Consequently, Zhang and Liu [19] have presented hydrogen liquefaction based on 4 refrigeration cycles including one nitrogen and 3 MRs cycles. As per sensitivity analysis, the optimal SEC was reported as

5.742 kWh/kg LH_2 with exergy efficiency of 55.30%.

It is important to note that the above mentioned LH_2 process models cannot be compared with one another as they all differ in process configuration and results in different SEC and exergy efficiency values [20]. Furthermore, these process models largely depend on their relative H_2 capacities where selection of refrigerants has a key role in demonstration of overall energy consumption and LH_2 process efficiency. This is the reason that recently proposed processes largely differ in energy perspectives. Beside all, the process complexity of existing models with the selection of multi-refrigerants in a single cycle is another factor which can be a main obstacle in commercialization. As discussed earlier, the MRs used in refrigeration cycles can reduce the overall energy consumption where precooling cycle is highly energy intensive however, the energy gap is still huge due to the fall in a very low temperature such as precooling is required to achieve −159.4 °C (25 °C base temperature) using a single cryo–exchanger [17]. Moreover, the conversion of Para state is one of the most crucial factors because of LH_2 product stability. Considering the above challenges such as energy intensive nature, process complexity, Ortho to Para conversion, thermodynamic efficiency, and exergy efficiency, we have made an effort to propose a simple, an energy and, cost efficient LH_2 process based on four refrigeration cycles with unique selection of MRs. The proposed model is compared in energy and exergy aspects with the commercial model and with the model developed by Qyyum et al. [17] which will serve as a base case–I and base case–II, respectively. The proposed study is compared with the base case designs in terms of energy, composite curve, exergy, economic and thermodynamic analysis.

2. Problem statement

Owing to a very low boiling point temperature (−252 °C) and isomer spinning (ortho to para conversion), liquefaction of H_2 consumes enormous amount of energy which makes it an energy–intensive process. In the base case–I and II [17], LH_2 process consists of three refrigeration cycles:

- Precooling cycle (25 to −153 °C) – MRs (methane, ethane, propane, n-butane, iso-butane, and nitrogen)
- Cooling cycle (−153 to −235 °C) – MRs (methane, ethane, propane, nitrogen, hydrogen)
- Liquefaction cycle (−235 to −252 °C) – Refrigerants (helium and hydrogen)

As per thermodynamic analysis performed on the model developed in the base case designs, it was predicted that the energy consumption was reduced from 10.15 kWh/kg LH_2 (base case–I) to 6.45 kWh/kg LH_2 (base case–II) after process optimization [17]. The efforts were made to reduce the energy consumption of precooling cycle of the base case–I which was recorded as 6.97 kWh/kg LH_2 including 68.7% of overall SEC of the LH_2 process. The obtained results after process enhancement revealed that the precooling cycle energy was reduced to 4.53 kWh/kg LH_2 in base case–II [17]. However, even after process enhancement and optimization, the total share of energy consumption by precooling cycle still stayed with 70% which is mainly due to large drop in temperature (−153 °C) through a single cooling loop. Moreover, exergy destruction values were found to be higher in respective precooling cycles. In base case–I and II, the exergy destruction values were calculated as 4.7 and 3.18 kWh/kg while total were 9.27 and 6.13 kWh/kg, respectively. The higher values of exergy destruction across precooling cycle may be due to insufficient heat exchange between hot and cold streams passing through cryogenic heat exchanger. Figs. 1 and 2 present the heat flow and temperature profiles of base case designs across the first exchanger where precooling temperature is achieved through MRs based precooling cycle.

The potential savings can be seen through the composite curve analysis performed in base designs such as the height of temperature difference composite curve (TDCC) depicts the inefficient heat transfer, as shown in Figs. 1 and 2**.** The high energy gap between hot and cold composite curves compel to shift the attention towards the selection of MRs with more suitable flow rates to reduce the gaps for example the highest energy loss is recorded in a temperature range of 25 to −30 °C. In addition, the precooling cycle has a high load to reduce the temperature from 25 to −153 °C which clearly means that the unique selection of high boiling refrigerants is required to achieve the corresponding temperature range. However, as per authors' understandings, the factor of complexity will increase upon addition of more refrigerants based on certain temperature ranges in a precooling cycle. Therefore, to cope with energy and exergy loss issues, we have proposed a LH_2 model with four cooling cycles such as;

- Precooling cycle-I (25 to −30 °C) – MR (HFO-1234yf hereafter as HFO, ethane, propane, n-butane, and iso-butane)
- Precooling cycle-II (−30 to −159.4 °C) – MR (methane, ethane, n-butane, and nitrogen)
- Cooling cycle (−153 to −235.2 °C) – MR (methane, ethane, propane, nitrogen, hydrogen)
- Liquefaction cycle (−235 to −252 °C) – Refrigerants (helium and hydrogen)

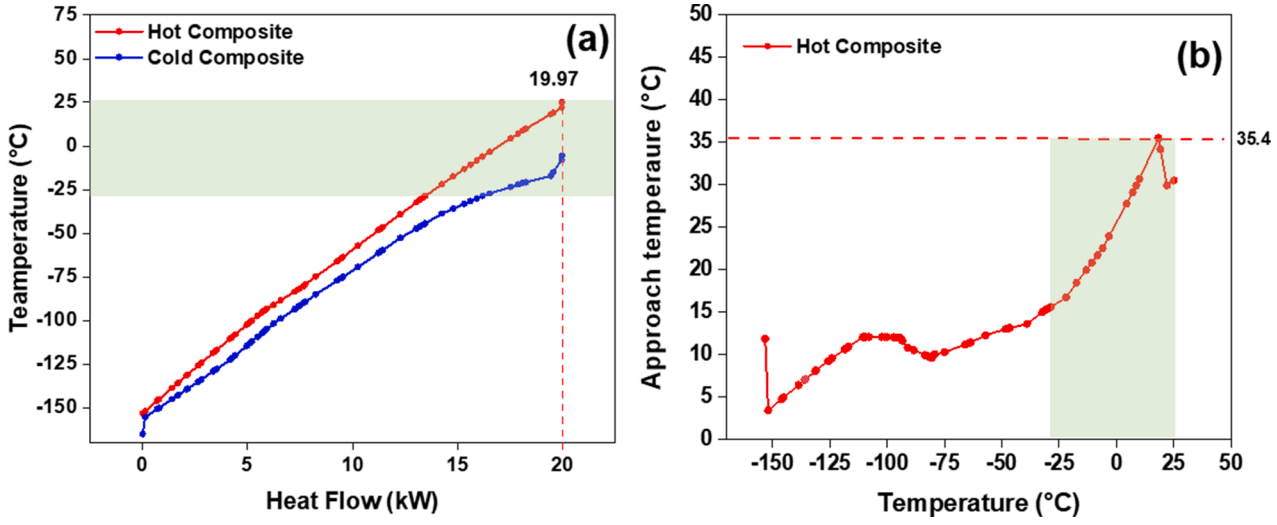


Fig. 1. Temperature heat flow composite curve and temperature difference composite curve of base case–I with SEC of 10.15 kW/kg LH_2.

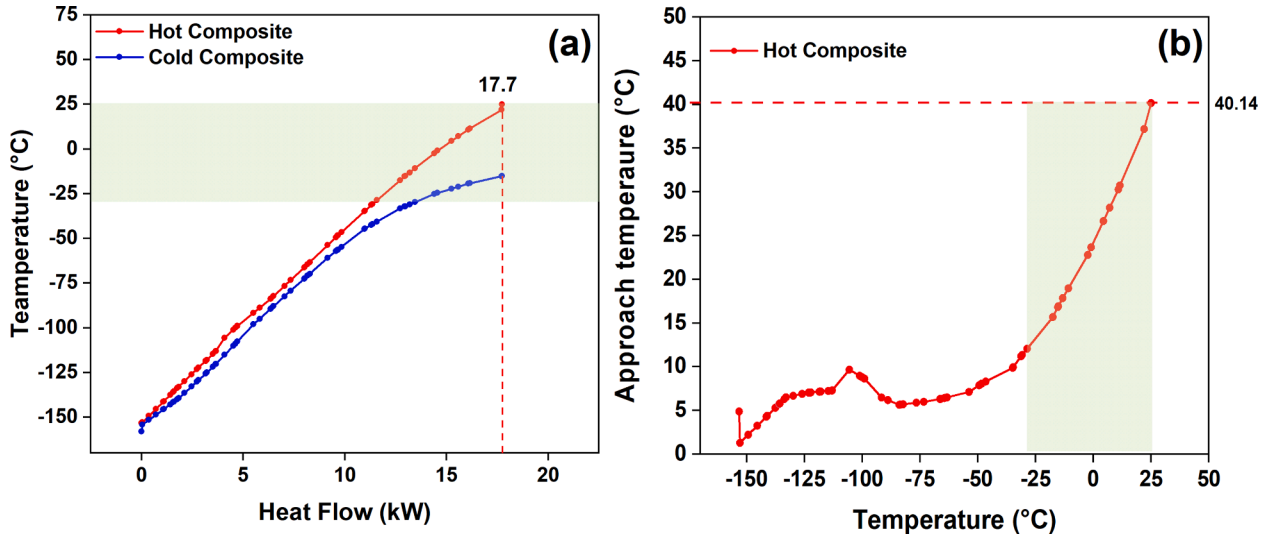


Fig. 2. Temperature heat flow composite curve and temperature difference composite curve of base case–II with SEC of 6.45 kW/kg LH_2.

In contrast to base cases, proposed process is further enhanced by considering an additional reaction system equipped with final exchanger to enhance the conversion of para–H_2 up to $\geq$ 99.5%. The addition of an extra cooling cycle results in less energy demand and more efficient LH_2 process. In precooling cycle–I of proposed process, HFO is introduced with other hydrocarbons to reduce the energy consumption (29.5%) of the hydrogen liquefaction process. This is because, by adding HFO (BP: −29 °C), the gap between the boiling points of propane (BP: −42.04 °C) and iso-butane (BP: −11.7 °C) is fulfilled, which ultimately helps in reducing the entropy generation and energy consumption.

The application of HFO has also been analyzed in the liquefaction process of NG [21]. HFO in the precooling of NG was used and ~ 46.4% energy savings were achieved as compared to single-loop MR process. As reported in many studies [22] that the HFO has a zero ozone depletion potential (ODP) [23] and low global warming potential (GWP) [24] that is why its use as a refrigerant is increasing especially, in air conditioning systems. Owing to have potential benefits in energy savings and eco-friendly nature, HFO in combination with C_2H_6, C_3H_8, n-C_4H_{10}, and i-C_4H_{10} is proposed in current study as a MR to achieve the target temperature values of H_2 feed (−30 °C) through a precooling cycle–I. Table 1 enlists the basic thermodynamic and environmental parametric values of each component in the proposed HFO–MR hydrogen liquefaction process.

3. Process design approach

3.1. Process simulation

The proposed LH_2 process is simulated in commercial software Aspen HYSYS V11. The thermodynamic properties of each refrigerant and H_2 is retrieved from software's library by selection of vast database property method Peng Robinson (PR) equation of state due its high accuracy over wide ranges of temperature and pressure [25]. The additional refrigerant, HFO, is retrieved from Aspen Plus V11 library as it is not available in HYSYS database. Since, proposed case is enhanced on the basis of existing literature [17] so, the design basis are kept same for fair comparison with the base case. The feed is combination of two isomers of H_2, 75% Ortho-H_2 and 25% Para-H_2 by mole, fed in cryogenic exchangers system at 25 °C and 21 bar. The other process assumptions are as follows;

- Pressure drop across cryogenic heat exchangers and coolers are assumed to be zero throughout the process
- Minimum temperature approach (MITA) across all heat exchangers is in the range of 1–3 °C
- Pressure ratio in multi–compressors is $\leq$ 3.0
- Adiabatic efficiency of compressors is 80%
- Isentropic efficiency of expanders is assumed to be 80%

Table 1
Thermo-physical properties of HFO with conventional mixed refrigerants [21].

Properties	Ethane	Propane	HFO	n-butane	i-butane
Mol. Wt.	28.05	42.08	114	58.12	58.12
BP (°C)	−88.6	−42.0	−29	−0.5	−11.7
Tc (°C)	32.1	96.9	94.7	151.9	135
Pc (bar)	48.72	42.48	33.82	37.96	36.48
ODP	0	0	0	0	0
GWP	6	3	4	4	3

3.2. Ortho to para conversion (OPC)

H_2 exists in two forms of isomers indicated by spinning of H_2 atoms. Para–H_2 is identified when both nuclei spin with the same direction and Ortho–H_2 is identified when both nuclei spin with the opposite direction as shown in Fig. 3. Generally, H_2 at 25 °C consists of 25% Para–H_2 and 75% Ortho–H_2. Ortho to Para–H_2 conversion (OPC) is temperature dependent, and 99.0% concentration of Para–H_2 is achieved when the temperature is reduced to liquefaction temperature of H_2 (20 K) under catalytic environment. The enthalpy of Ortho–H_2 is 527 kJ/kg, which is higher than the Para–H_2 form (447 kJ/kg). Consequently, OPC is exothermic reaction that enhances the total reversible work thus more energy is required to achieve the liquefaction temperature of H_2. Thus, the OPC is one of the most important aspects needs to be considered while designing LH_2 process and equally important from storage point of view.

OPC is very slow 2nd order reaction which takes > 2 months to convert from 25% to 95% Para–H_2. This slow exothermic conversion makes enough heat to vaporize 50% of H_2 in 10 days if the H_2 is stored without maintaining equilibrium [26]. This boil–off phenomenon tends to vaporize the H_2 with the rate of 1% h^{-1} (18% d^{-1}). However, boil–off associated with H_2 can be prevented by keeping the H_2 into liquefied Para–H_2 isomer form because of its stability. This is the reason that commercial liquefiers are operated to achieve $\geq$ 95% Para–H_2 form [8]. Moreover, catalytic activity starts after precooling step where catalyst is embedded inside the cryogenic exchangers on H_2 side. The placement of catalyst inside the exchangers has significant importance because the

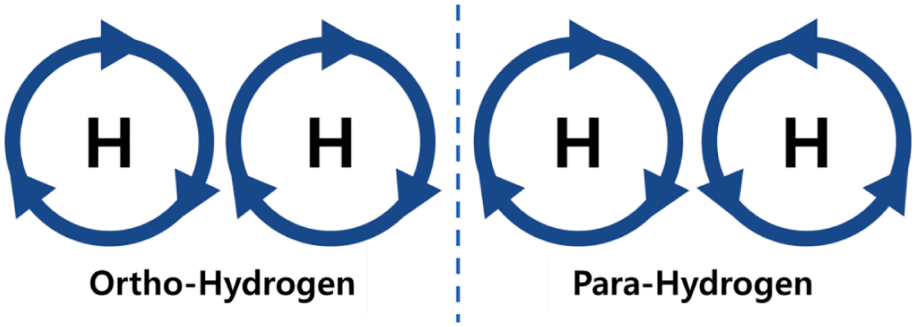


Fig. 3. Spin motion of ortho– and para– isomers of H_2.

heat emission during catalytic conversion can be well managed during cryogenic heat exchanging operation otherwise it causes the evaporation of liquid H_2 [27]. Commercially, catalysts like iron–oxide ($Fe_2O_3.2\%H_2O$, IONEX®) or Chromium oxide–silica doped ($C_rO.SiO_2$, OXISORB®) are currently used for controlling the speed of OPC and making high conversion rate with competitive performance and cost [27]. In current study, OPC is carried out through IONEX®. The following equations (I and II) represents the chemical reaction of OPC with catalyst. Where *A* represents the catalyst.

$$2\mathrm{A} + \mathrm{o} - H_2 \rightarrow 2\mathrm{A}H_2 \rightarrow 2\mathrm{A} + \mathrm{p} - H_2 + \Delta\mathrm{H} \quad \text{(I)}$$

$$\mathrm{o} - H_2 \rightarrow p - H_2 + \Delta H \quad \text{(II)}$$

Commercial simulator Aspen needs the kinetic data to support OPC reaction however, the required information of kinetic parameters is unavailable in open literature. In this context, efforts have been made by researchers to estimate the conversion associated with composition profile based on equilibrium which can be determined through equation III.

$$\mathrm{Conversion}(\%) = C_0 + C_1 \times T + C_2 \times T^2 \quad \text{(III)}$$

where,

C_0, C_1 and C_2 = conversion coefficients.

T = H_2 temperature (Kelvin).

Thus, based on equation (III) conversion reactors in HYSYS were operated to achieve OPC. Fig. 4 represents the ortho to para conversion profile across temperature. Coefficients of conversion for each reaction system were estimated from the experimental data [28–30] which is fitted in such a way that the conversion of Para–H_2 against temperature corresponds to the exactly experimental values at the outlet of each reactor. It is important to mention that the realistic conversion values may differ with these predictions however, this technique has been used in many studies [17,18,31] to compute the conversion values for embedded reaction systems of hydrogen liquefaction.

3.3. Process description

Hydrogen liquefaction is mainly consisted of three refrigeration cycles, named as precooling, cooling, and liquefaction. Each cycle is the combination of compression and interstage cooling system with cryogenic heat exchanging devices as shown in Fig. 5. To cover a large temperature gap in the first heat exchanger of the base case, a new refrigeration cycle with HFO-MR is introduced as a precooling cycle-I to bring the temperature of H_2 stream from 25 to −30 °C. Thus, the proposed case has two precooling cycles which reduce the temperature of H_2 (−159.4 °C) into two stages as precooling cycle–I and precooling

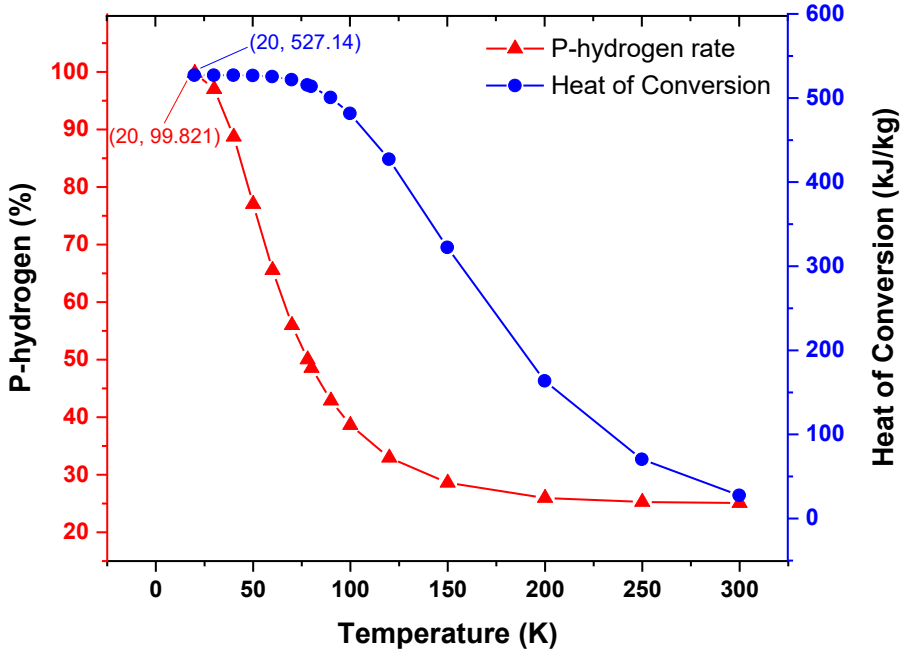


Fig. 4. Para–H_2 rate and heat of conversion profile along temperature [28–30].

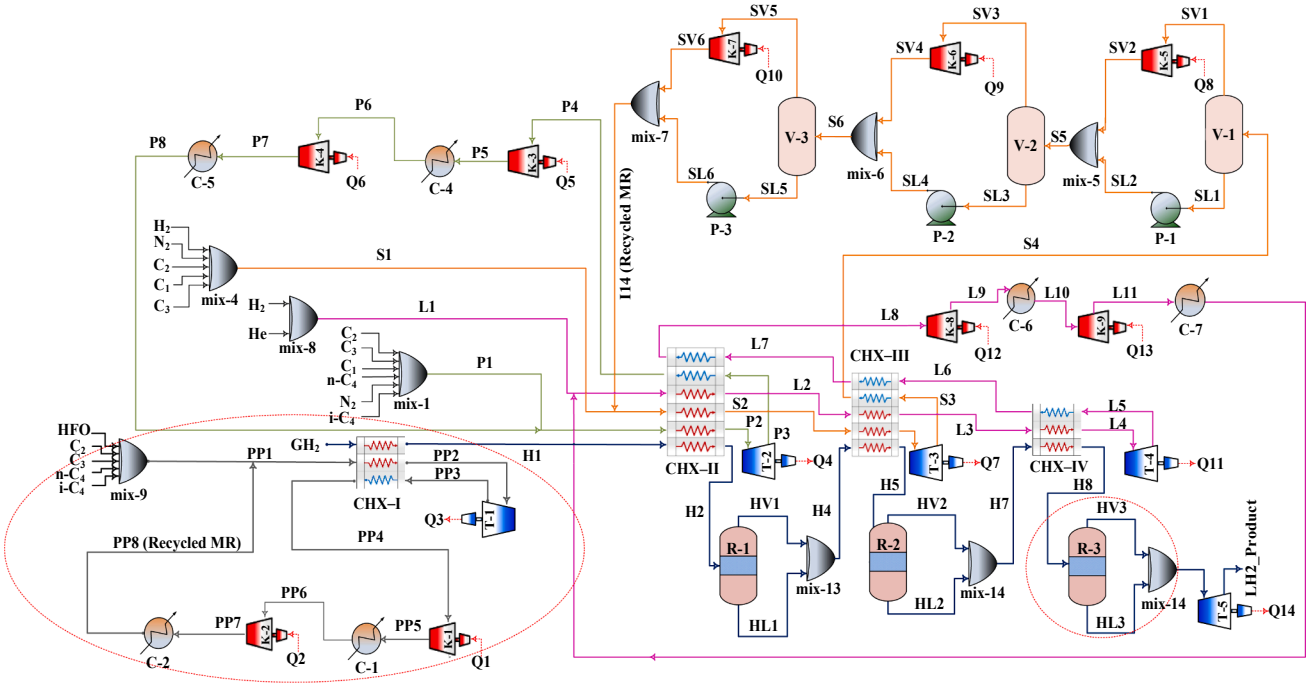


Fig. 5. Schematic of proposed hydrogen liquefaction process.

cycle–II. Since, the proposed case is the enhancement of base case [17] so, the cooling and liquefaction cycle contain same refrigerants with varying flow rate and operating conditions to achieve an optimal solution. The proposed H_2 liquefaction process was modeled with four refrigeration cycles.

Mixed refrigerant stream (stream PP1) which consists of C_2, C_3, n-C_4, i-C_4, and HFO is used to drop down the temperature of GH_2 after cryogenic heat exchanger (CHX-1). The stream used as a cold medium PP1 is first compressed in a 2-staged compression and interstage cooling system to increase the pressure by 25.55 bar and then introduced into CHX–1. After exchanging heat with hot stream, PP2 is depressurized to 4.1 bar in an expander (T-1). The expansion of refrigerant stream results in a temperature decrement of −42 °C. The expanded stream PP3 is reintroduced into CHX–1 and exchange heat with GH_2 to drop its temperature by −30 °C. The precooled stream of gaseous H_2 is discharged to CHX–II where precooling cycle–II tends to reduce its temperature to −159.4 °C. The precooling cycle–II comprising of another MR stream containing C_1, C_2, C_3, n-C_4, and N_2 is compressed from two staged compressors system. The hot stream exiting from compressors were coupled with interstage cooling system to reduce the temperature of refrigeration stream. The discharge pressure of MR stream used in precooling cycle–II is obtained as 12.5 bar after process optimization while suction pressure after expansion of MR stream is calculated as 1.56 bar with resulting temperature of –161.1 °C. The expanded stream after passing through the CHX–II is pushed to compression and cooling system in order to complete the refrigeration cycle. The stream P5, exiting from CHX–I, is compressed to 4.416 bar by compressor K–4 and cooled down to 22.0 °C by aftercooler. Consequently, the stream P7 is compressed to 12.50 bar and cooled down to 22.0 °C, same condition with the feed stream of precooling cycle. Since, ortho to para conversion of H_2 is slow process therefore, first reaction system is equipped with CHX–I to increase the reaction rate that results in ~ 35% conversion of Para–H_2 at −159.4 °C.

Fully precooled stream of GH_2 is then charged to CHX–III where cold duty of cooling cycle is used to drop down the temperature of H_2 stream by 235.2 °C. The refrigerant stream of cooling cycle is initially passed through CHX–II to reduce its temperature to −159.4 °C and then cold stream S2 is introduced in CHX–III where heat is exchanged in countercurrent way facilitated with T–3 expander, temperature reduction −238.3 °C and S4 sent back to CHX–III. The suction and discharge pressure of cooling cycle is 4.1 bar and 36.2 bar, respectively. Second reactor is equipped with CHX–III to facilitate the further conversion of para–H_2 (89.3%). The feed stream of Liquefaction cycle is cooled to −159.4 °C in the cryogenic heat exchanger CHX–II and introduced to CHX–III and cooled to −235.2 °C. The stream L3 is introduced to −251.8 °C in the cryogenic heat exchanger CHX–IV and expanded from 25.0 bar to 3.9 bar which results in decrement of temperature up to −252.9 °C. The stream L5 is used as a cooling medium in the cryogenic heat exchanger CHX–IV and heated to −236.6 °C. The stream L6 is heated to −160.5 °C in the cryogenic heat exchanger CHX–III and introduced to CHX–II as a cooling refrigerant and heated to −32.0 °C. The H8, hydrogen stream, achieved a temperature of −251.8 °C in the cryogenic heat exchanger CHX–IV and fed to reactor (R–3) to get 99.52% para–H_2.

4. Process analysis

The proposed process is compared with the base case design based on energy, exergy, and composite curve analysis. The description of individual analysis is presented separately in subsection.

4.1. Energy analysis

Typically, LH_2 processes are highly energy intensive, mainly due to the fact of high energy consumption incurred by compressors. Specific energy consumption (SEC) is the most useful parameter, based on that energy analysis are carried out to predict the efficiency of the process. The SEC is basically dependent on type of refrigerants, their flow rates, composition, and operating pressures in LH_2 process. Therefore, in current study, we have chosen the aforementioned parameters as design variables to predict their potential impact on SEC. In addition, the temperatures of precooling and cooling cycles were also considered as variables in proposed design. Mass flowrates of refrigerants used in base case–I, base case–II, and proposed case are presented in the Table 2.

Since, precooling cycle in base case designs covers a large range of temperature that ultimately results in a high energy consumption

Table 2
Comparison of mass flowrate of refrigerant used in base case I, base case II and proposed case.

Refrigerants	Base Case–I	Base Case–II	Proposed Case
Precooling cycle–I	*(kg/h)*		
C_2	–	–	1.08
C_3	–	–	0.83
i–C_4	–	–	0.29
n–C_4	–	–	0.15
HFO	–	–	0.15
Total	–	–	2.5
Precooling cycle–II			
C_1	25.80	14.0	9.85
C_2	27.36	21.81	10.0
C_3	24.90	4.50	0.45
i–C4	11.41	15.25	–
n–C_4	22.00	28.36	34.0
N_2	5.75	0.78	1.15
Total	117.22	84.7	55.45
Cooling Cycle			
C_1	5.70	1.12	1.20
C_2	12.00	3.60	1.10
C_3	14.00	25.36	25.20
H_2	1.65	1.48	1.24
N_2	8.0	1.46	2.95
Total	41.35	33.02	31.69
Liquefaction cycle			
H_2	2.25	1.75	1.75
He	1.56	0.15	0.14
Total	3.81	1.90	1.89

therefore, dividing the precooling load in to two cycles (precooling–I and precooling–II) makes refrigerant selection more impactful. As a result, SEC of the proposed case is reduced to 4.55 kWh/kg LH_2 and energy savings approach to 55% and 29.5% as compared to base case–I and base case–II, respectively. The reduction in energy consumption is because of reducing the overall refrigerants flow rate such as precooling cycle–I requires only 2.5 kg/h of refrigerants with the unique selection of refrigerants where n–C_4 and i–C_4 are low boiling point while HFO, C_2, and C_3 are high boiling point refrigerants used to precool the gaseous H_2 up to −30 °C. Consequently, precooling cycle–II plays a central role to achieve the precooling temperature of −159.4 °C with the selection of mixed refrigerants. The mixed refrigerant is advantageous for the cryogenic heat exchanger because of providing enough refrigeration capacity with wide boiling point range and high thermodynamic efficiency. Hence, overall flow of refrigerants in precooling cycle is reduced to 50.6 and 31.6% as compared to base case–I and base case–II, respectively. Importantly, the higher flow of n–C_4 in proposed case is thermodynamically suitable for high refrigeration capacity of precooling cycle to achieve a certain goal of precooling temperature. In addition, the precooling temperature (−159.4 °C) is enhanced with optimal selection of pressure ratio (2.83) inside the multi–compression system, suction (1.56 bar) and discharge pressure (12.5 bar) of refrigerants stream. Considering the power factor incurred in precooling section, proposed case utilizes 2.83 kW of power which is 51% and 32.6% less than utilized in base case–I and base case–II, respectively.

Similarly, process enhancement in base case design is more impactful in cooling cycle. The mixed refrigerant stream includes C_1, H_2, and N_2 high boiling point liquids which tend to reduce the temperature of gaseous H_2 by −235 °C. However, existence of high boiling components such as C_2 and C_3 results in a high specific refrigeration effect, generally depends on the concentration of refrigerants with critical temperature close to ambient temperature. Therefore, cooling cycle has 79.5% share of C_3 in MR stream. The overall refrigerants flow is observed to be reduced to 23.4% and 4% as compared to base case–I and base case–II, respectively. Furthermore, suction pressure is increased to 4.1 bar which ultimately reduces the load on compressors thereby decreasing the SEC. As per power consumption perspective, the proposed case leads with the 62.7% less energy consumption in cooling cycle as compared to base case–I. Consequently, 38.7% power reduction is observed in proposed case when compared with base case–II.

In the liquefaction loop, H_2 and He are used as a cooling medium having a mass flow of 1.89 kg/h. The suction and discharge pressure were optimized with MITA value of CHX–IV at 1.011 °C. The mass flowrate of H_2 is decreased up to 50.4% compared to base case–I because the temperature gap that CHX–III needs to cover is decreased from 24 °C to 17 °C. This is the reason that total energy required in liquefaction cycle is reduced to 53% and 15% when compared with base case–I and base case–II, respectively. As reported in Table 3, the total compression power is reduced by 53.6% as compared to base case–I while overall power generated through expanders were obtained as 0.465 kW in proposed case.

4.2. Composite curve analysis

The composite curve is thermodynamic graphical tool for analyzing the refrigerants behavior and presents the process overview over specific heat and temperature ranges in a multi–stream heat exchanger device. These curves show a relation of heat exchange between hot and cold streams across the cryogenic heat exchangers. The temperature heat flow composite curves (THCCs) demonstrate the change in temperature between hot and cold composite against heat flow within a heat exchanger while temperature difference composite curves (TDCCs) Another type of composite curve relates temperature to approach temperature (MITA). The gap between the composite curves can be used to

Table 3
Comparison of design variables and specific energy consumption among base case I, base case II and proposed case.

Design Variables	Base case I	Base case II	Proposed case
Precooling cycle–I			
Suction pressure P_{PR3}, (bar)	–	–	4.1
Discharge pressure $P_{PR\text{-}14V}$, (bar)	–	–	25.55
Pressure ratio	–	–	2.35
Pre-precooling temperature T_{H1}, (°C)	–	–	–30
Precooling cycle–II			
Suction pressure P_{P3} (bar)	2.5	1.52	1.56
Discharge pressure $P_{P\text{-}10V}$ (bar)	19.5	13.0	12.50
Pressure ratio	2.79	2.92	2.83
Precooling temperature T_{H2} (°C)	–153.2	–153.20	–159.4
Cooling cycle			
Suction pressure P_{I4} (bar)	2.5	2.98	4.1
Discharge pressure $P_{I14\text{-}V}$ (bar)	41.7	35.60	36.20
Pressure ratio	2.56	2.29	2.07
Cooling temperature T_{H5} (°C)	–240.4	–240.4	–235.2
Liquefaction cycle			
Suction pressure P_{S5} (bar)	3.8	3.75	3.9
Discharge pressure P_{S11} (bar)	20.0	25.0	25.0
Pressure ratio	2.294	2.58	2.532
Cooling temperature T_{H8} (°C)	–251.8	–252.8	–251.8
Constraints			
$MITA(X)_{CHX\text{-}I}$ (°C)			2.671
$MITA(X)_{CHX\text{-}II}$ (°C)	3.107	1.085	1.140
$MITA(X)_{CHX\text{-}III}$ (°C)	3.067	1.063	1.013
$MITA(X)_{CHX\text{-}IV}$ (°C)	3.329	1.004	1.011
Total compression power (kW)	10.81	7.027	5.013
Power generated (kW)	0.66	0.577	0.465
Net power (kW)	10.15	6.450	4.55
SEC (kWh/kg_{LH2})	10.15	6.450	4.55

explain the entropy generation and results in exergy loses. Since, proposed case contains four refrigeration cycles and has different process configuration compared to base case designs to liquefy H_2, therefore, Fig. 6 represents THCC of all four cryogenic heat exchangers. Fig. 6 (a) demonstrate the heat flow across temperature in CHX–I, the large gap between hot and cold composite curves is due to the occurrence of partial change in phase of refrigerants stream inside the cryogenic heat exchanger. This phase change tends to utilize the sensible and latent heat of MR however, the gap between curves also signifies the flexibility of precooling cycle–I with unique selection of refrigerants. As MITA value inside CHX–I is kept higher (2.671 °C) than 1 °C so, this pinch point significantly mentions about the optimal selection of refrigerants composition. However, HFO in precooling cycle–I is opted to reduce the energy losses during the initiation of liquefaction process specifically, for precooling section where temperature ranges from 25 °C to −30 °C.

Fig. 6 **(b)** shows the THCC of CHX–II for precooling cycle–II. From −30 to −159.4 °C, the narrow gap between cold and hot composite curves exhibits the optimal selection of MR and their appropriate heat exchange which point out the very low or negligible entropy generation in CHX–II. Nevertheless, it can be clearly seen that the curves have deviation when temperature is ≥ −30 °C. This gap may be the result of phase change of high boiling refrigerants caused due to evaporation pressure. This gap can be reduced upon increasing of evaporation pressure but will results in low MITA < 1 °C. Also, it is important to mention that varying the composition of high boiling refrigerants (C_2, C_3, and n-C_4) in precooling cycle–II largely effect the SEC and MITA value.

Similarly, Fig. 6 **(c)** shows THCC behavior between hot and cold composite curve in CHX–III. Owing to the presence of N_2 and H_2, the very narrow gap between composite curves was observed at the corners which depicts the high energy efficiency and less entropy generation across CHX–III. However, the middle section has some gap between curves that is due to the presence of high boiling components such as C_2 and C_3 which undergoes phase change upon reduction of temperature inside the heat exchanger. Nevertheless, presence of C_2 and C_3 largely effect the overall energy consumption of process.

Finally, THCC of CHX–IV is shown in Fig. 6 (d), wide gap between hot and cold composite curves reveals that the design variables can be further optimized to reduce the gap. The flow of H_2 in liquefaction cycle largely effects the gap, increasing the flow of H_2 can reduce the gap from the hot end but the overall SEC will be increased. On the other hand, decreasing the flow of He results in low energy gap at cold end of THCC. However, there is always a tradeoff among the selection of refrigerants and their corresponding flow to be used for the reduction of energy and exergy destruction.

In proposed case, the TDCC of cryogenic heat exchangers are shown in Fig. 7 while Fig. 8 presents the TDCC of base case–I, base case–II, and proposed case for the sake of comparison and the potential benefits achieved after process enhancement (proposed case). All the curves presented in Fig. 8 are within the MITA constraint limit 1–2 °C. Only CHX–I of the proposed case has 2.671 °C, TDCC of CHX–I for proposed case is above 0 °C and the gap between composite curves is low that ensures the thermodynamic feasibility with MITA value reaching at 27.94 °C. However, the high height of the curves comprehends the potential energy savings with the optimal solution of design variables. Also, the phase change occurrence results in high energy gap that can be

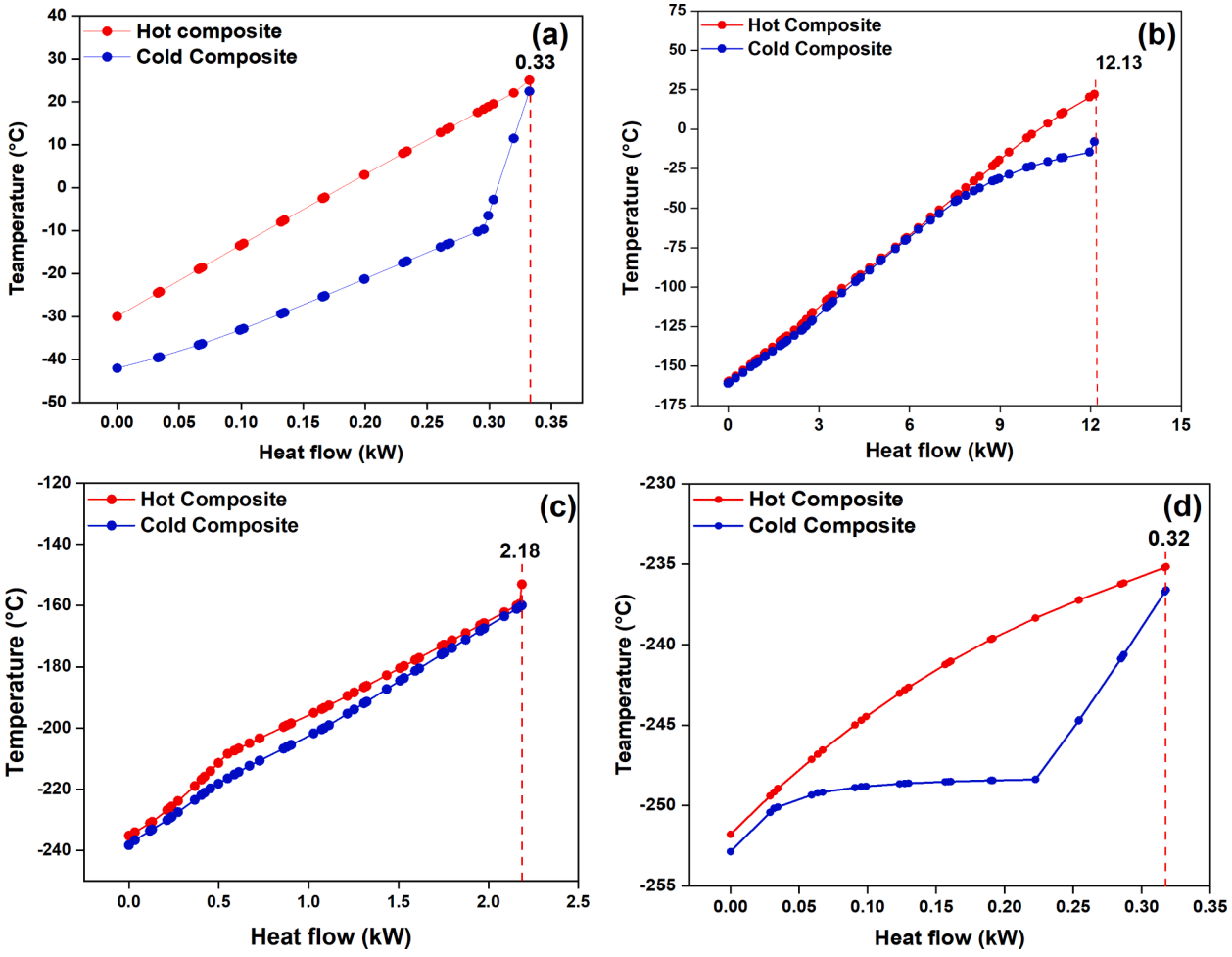


Fig. 6. Temperature heat flow composite curves of CHX–I, CHX–II, CHX–III, and CHX–IV of proposed case.

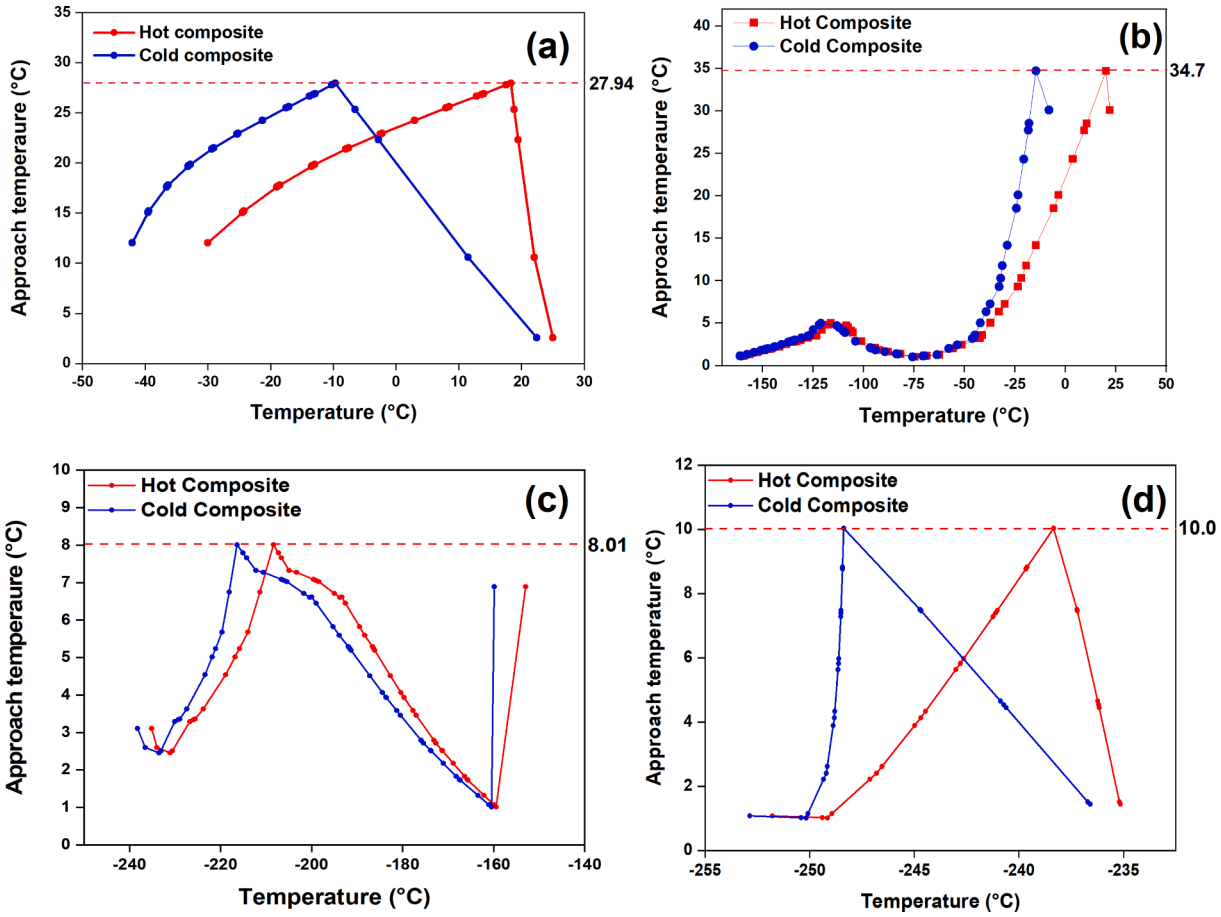


Fig. 7. Temperature difference composite curves of a) CHX–I, b) CHX–II, c) CHX–III, and d) CHX–IV of the proposed case.

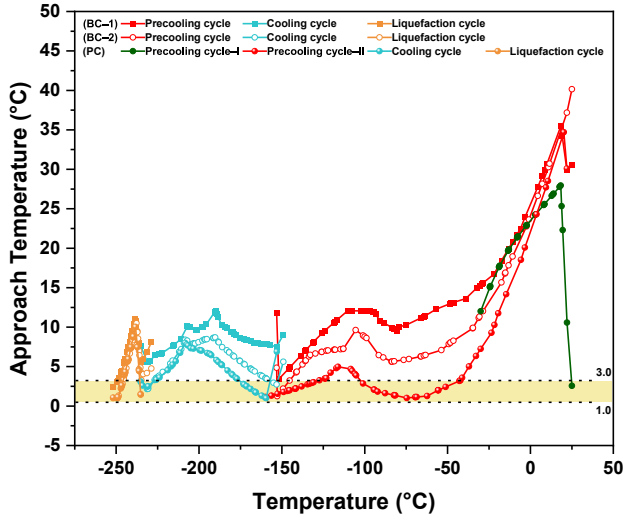


Fig. 8. Temperature difference composite curves of base case–I, base case–II, and the proposed case.

overcome by increasing the flow of refrigerants, suction, and discharge pressure however, the MITA and SEC in a result is observed to be high that leads to low energy efficiency. Consequently, the precooled gaseous H_2 further passed through CHX–II to achieve the target precooling temperature of −159.4 °C where TDCC of respective heat exchanger exhibits very low energy gap. The height attained by curves is even lower than base case design which results in low entropy generation but shows distinct gap at top extreme edges of composite curves where MITA value approaches to 34.7 °C. The sharp turn is obtained at highest peak where phase change of high boiling liquids exists. This high MITA reveals that the energy saving opportunities are still available with the adjustment of design variables. Similarly, TDCC of CHX–III depicts sharp turn in the middle of curves in between −220 and −210 °C and, the highest value of MITA 8.01 °C is observed at the same point. The peak of TDCC of liquefaction exchanger is obtained at 10 °C and approaches the MITA constraint at 1.011 °C.

According to Fig. 8, the proposed case exhibits better demonstration of heat recoveries within heat exchanging systems. It can be clearly seen that the TDCC peak attained by CHX–II of proposed case is lower than precooling exchanger of base case which is due to the fact of liquefaction cycle stream entering at lower temperature −123.8 °C, MITA will be low when temperature difference between cold and hot stream is low. This is the reason that better heat recoveries are obtained in the range of −40 to −160 °C and the MITA remains lower than 5 °C. Similarly, performance of CHX–III of proposed case is higher as compared to both base cases due to the attaining of less peak height for MITA (8.01 °C). Also, there is an interesting temperature increment is seen at hot end of exchangers CHX II–IV due to exothermic ortho to para conversion of H_2 isomers. Unlike base case–I and II, the R–3 is coupled with CHX–IV to achieve the purity of para–H_2 up to 99.5%. However, there are some energy losses observed and the abrupt change in peak of CHX–IV due to addition of an extra reaction system.

4.3. Exergy analysis

Quantification of exergy is an essential thermodynamic tool to assess the efficiency of the process. Source of reversibilities and thermody-

namic inefficiencies of the processes can easily be located through exergy analysis. Exergy can be in different forms such as physical, chemical, kinetic, and potential exergy. Based on steady state system, kinetic and potential exergies can be neglected in current study. The physical and chemical exergies are expressed as Equation IV and V.

$$ex_{ph,i} = (h_i - h_0) - T_0(s_i - s_0) \quad \text{(IV)}$$

$$ex_{ch,i} = \sum x_i e_i^{CH} + RT_0 \sum x_i ln x_i \quad \text{(V)}$$

where, $ex_{ph,i}$ and $ex_{ch,i}$ are the physical and chemical exergies and h and s denote the enthalpy and the entropy, respectively. The x_i denotes the mole fraction of component i. The e_i^{ch} denotes the standard exergy of the component i. Exergy destruction for the equipment is calculated using equations shown in Table 4. The exergy efficiency (μ_{ex}) of LH_2 process can be calculated as Equation VI.

$$\mu_{ex} = \frac{(E_{xproduct}) - (E_{xFeed})}{W_{total}} \quad \text{(VI)}$$

Specific exergy destruction of base case I, base case II and propose case were determined on basis of studied processes and their comparison is listed in Table 5. From Table 5, it can be clearly seen that the overall exergy destruction of proposed case is very less than base case designs. Therefore, it can be mentioned that the higher heat recoveries were obtained from refrigeration loops with less entropy generation in proposed case. Among all equipment, phase separators share a larger contribution in overall exergy destruction as 49.6% following the expanders (28.8%) and compressors (27%). However, exergy destruction follows a specific trend as separators > compressors > expanders > coolers > reactors > pumps based on contribution of each equipment in base case–I and base case–II except heat exchangers. As a result, the proposed case has 60% and 39.5% exergetically more powerful when compared with base case–I and base case–II.

Fig. 9 represents the specific exergy destruction across the heat exchangers of base cases and proposed case. The proposed design has shown −0.97 kWh/kg of exergy destruction. In comparison to base case designs, cryogenic exchangers in proposed design depicts low exergy destruction which is mainly due to the rigorous selection of MRs for wide range of temperature to efficiently exchange heat inside the heat exchangers. It is important to notify that the value of exergy destruction should not be a minus values. However, authors think that the resultant specific exergy destruction of CHX–III is negative due to the cascade design of refrigeration loops.

Exergy efficiency of a certain process is considered as a helpful criterion to compare the performance of the equipment in the process. Overall exergy efficiency of base case–I, base case–II and the proposed case are presented in the Fig. 10. The proposed case exhibits very high exergy efficiency, 30–55% when compared with base cases. The high exergy efficiency is because of the optimal selection of design variables especially, selection of appropriate refrigerants in each cycle. Consequently, the exergy destruction for compressor, expander and cryogenic heat exchanger is largely decreased as the precooling cycle–I decreases the load of the precooling cycle–II in temperature range from 25 to −30 °C that precooling cycle has to cool.

Table 6 enlists the quantified values of exergy destruction in each refrigeration cycle in base cases and proposed case. Splitting the precooling cycle results in a high energy efficiency and less exergy destruction such as the value of exergy destruction reduced to 1.51 kWh/kg. However, the exergy destruction of cooling cycle in proposed case is little bit higher (7%) compared to base case–II which is due to the occurrence of huge temperature difference between inlet and outlet streams in cryogenic exchanger. Undoubtedly, the overall exergy efficiency in proposed case is much higher because primary exchanger (CHX–II) facilitates all refrigeration loops in order to reduce the gap

Table 4
Equations used to calculate the exergy destruction across equipment.

Equipment	Exergy destruction (kW)
Compressor	$Ex_{des} = (m)(E_{in} - Ex_{out}) + W$
Aftercoolers	$Ex_{des} = (m)(E_{in} - Ex_{out})$
Cryogenic heat exchanger	$Ex_{des} = \sum(m)Ex_{in} - \sum(m)Ex_{out}$
Turbine	$Ex_{des} = (m)(E_{in} - Ex_{out}) - W$
Phase separators / Reactors	$Ex_{des} = (m)Ex_{in} - ((m)Ex_{Liq} + (m)Ex_{Vap})$

Table 5
Specific exergy destruction across equipment used in base case I, base case II, Proposed case.

Equipment	Base case I	Base case II	Proposed case
Compressors	2.06	1.73	1.00
Expanders	1.71	1.56	1.07
Pumps	0.05	0.03	0.03
Exchangers	1.71	–0.56	–0.97
Coolers	0.90	0.90	0.36
Phase separators	2.42	2.05	1.84
Reactors	0.42	0.42	0.38
Total	**9.27**	**6.13**	**3.71**

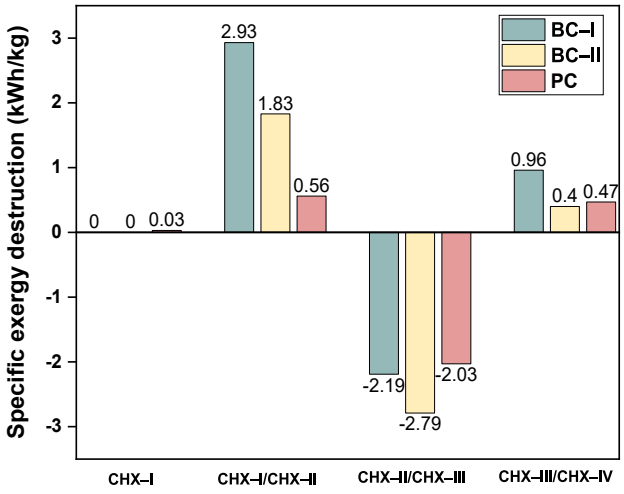


Fig. 9. Specific exergy destruction across heat exchangers of base case–I, base case–II, and proposed case.

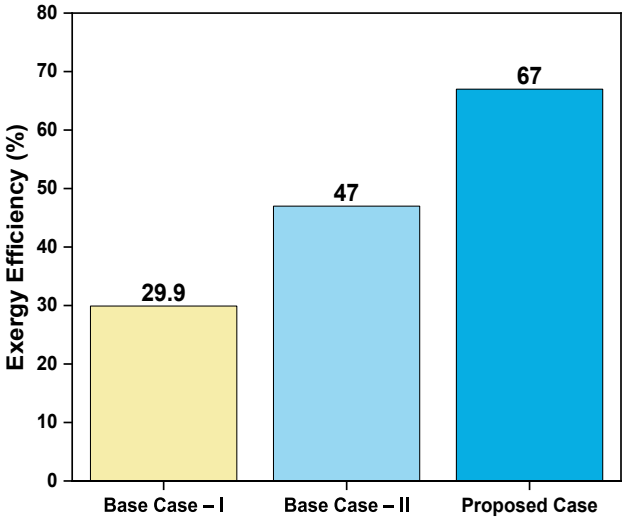


Fig. 10. Exergy efficiency of base case–I, base case–II, proposed case.

Table 6
Exergy destruction in the refrigeration cycles of the base case–I, base case–II, and the proposed case.

Refrigeration cycle	Base case–I	Base case–II	Proposed case
	(kWh/kg)		
Precooling cycle–I	–	–	0.06
Precooling cycle–II	4.7	3.18	1.45
Cooling cycle	2.54	1.3	1.4
Liquefaction cycle	2.03	1.63	0.76

between inlet and outlet streams of other exchangers. In other cases, the high exergy destruction is also due to the high energy loads require to meet the liquefaction temperature such as liquefaction loop of base case–I requires 50% more H_2 and He flow that ultimately increase the power consumption.

4.4. Thermodynamic efficiency

Thermodynamic process efficiency of proposed LH_2 model is calculated through coefficient of performance (COP) and figure of merit (FOM) relations. The COP of the process is calculated based on the relationship between the heat removal and the work required to remove the heat from the system. COP can be calculated based on the equation (VII),

$$\mathrm{COP} = \frac{\dot{m} \times (h_{GH_2} - h_{LH_2})}{W_{total}} \quad \text{(VII)}$$

In equation (VII), h_{GH2} and h_{LH2} represents the enthalpy of gaseous and liquid H_2, $\dot{m}$ mass flowrate of H_2, and W_{total} is the total required work for converting G–H_2 into L–H_2.

FOM indicates a relation of COP of LH_2 model in contrast to the ideal case. Performance of the proposed process is evaluated by the calculation of actual energy. The FOM is calculated as equation VIII.

$$\mathrm{FOM} = \frac{\dot{m} \times (Ex_{LH_2} - Ex_{GH_2})}{W_{total}} \quad \text{(VIII)}$$

where Ex_{LH2} and Ex_{GH2} represents the exergy of gas and liquid state hydrogen. Fig. 11 indicates the comparison of the base case–I, base case–II and proposed case according to calculated values of FOM and COP. Proposed process has 30% increase in FOM when compared with base case–II. Similarly, the COP was boost to 0.289 which is quite large than base case designs. Higher values of COP and FOM represent the high efficiency and manifest that the proposed process is exergetically stronger than base case designs. Moreover, less energy consumption and high exergy efficiency are the factors to elevate the thermodynamic efficiency.

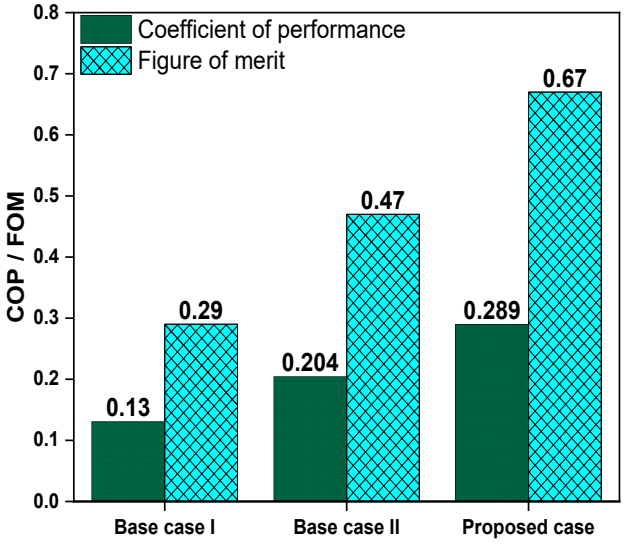


Fig. 11. Thermodynamic efficiency based on COP and FOM of base case–I, base case–II, and proposed case.

Furthermore, the proposed hydrogen liquefaction process is compared with the commercial scale and state of the art processes and found energy efficient than existing ones. Commercialized processes have relatively higher energy consumption within the range of 12–15 kWh/kg LH_2 as presented in Table 7. These higher SEC values are due to many factors such as GH_2 feed condition, product condition/composition (Para–H_2 percentage), type of refrigerants, type of heat exchangers and their pressure drops, and equipment efficiencies. In most of commercial scale processes, the cooling energy is obtained from single refrigerant such as LN_2 to precool the GH_2 [32]. In addition, commercial scale processes are not optimized in terms of energy aspects rather obtaining a liquid H_2 product is main objective. This is the reason that the exergy efficiency of current LH_2 processes is very low.

Compared to recently proposed conceptual designs as listed in Table 7, higher values of FOM and COP reveals that the proposed process has high thermodynamic efficiency and thus energy efficient. As discussed before, the MRs based LH_2 processes are attractive and energy efficient because the selection of refrigerants depends upon wide range of H_2 boiling point. However, there is no certain parameter to compare the existing processes as each process has different mechanism to obtain liquefied H_2. Nevertheless, process complexity is one of the critical aspects; existing processes are complex due to involvement of several equipment and refrigeration loops to get the similar objective which make them less attractive for commercial scale upgradation. Such structures are often avoided due to complex arrangement and interconnectivity of equipment [33]. On the other hand, proposed process is simple and utilized straight away four refrigeration cycles with similar arrangement and connectivity among process equipment.

4.5. Economic evaluation

Cost evaluation of proposed process is conducted to estimate the feasibility of the process in terms of its economic viability. In this regard, cost of new plant is estimated through rigorous calculation method provided by Turton et. al [39] based on module cost technique. Cost incurred by each item is calculated based on their capacity factors and their relevant equations and the details of capital cost (CAPEX) and operating cost (OPEX) are provided in Table 8. However, it is important to mention that the cost of cryogenic exchanger is crucial as special type of heat exchangers are required in cryogenic operations where a very

Table 7
Comparison of commercialized and state of the art LH_2 processes with proposed process.

LH_2 processes (Published references)	SEC (kWh/kg LH_2)	Exergy efficiency (%)	Figure of merit (FOM)	Coefficient of performance (COP)
Praxair [32]	12–15	19–24	–	–
Linde Ingolstadt [34–36]	13–15	21.2–22.2	–	–
Linde Leuna [37]	11.9	23.6	–	–
Zhang and Liu [19]	5.742	55.3	–	0.1574
Naquash et al. [38]	9.62	31.5	0.31	0.1
Qyyum et al. [17]	6.45	47.2	0.47	0.204
Asadnia and Mehrpooya [31]	7.69	39.5	0.39	0.17
Naquash et al. [18]	7.63	31.4	0.31	0.16
This process	4.55	67	0.67	0.289

Table 8
Equations used to calculate the overall economics of the proposed process.

Description	Cost calculation equations and relations [39–41]
Capital expenditures	
Equipment purchase cost (C_{EP})	$\log_{10}(\text{CEP}) = k1 + k2\log_{10}V + k3(\log_{10}V)^2$
Bare module cost (C_{BM})	$C_{BM} = E_p F_{BM}$
Capital cost of equipment (C_{EC})	$C_{EC} = 1.18\sum_i^n C_{BM,i}$
Capital recovery factor (C_{RF})	$C_{RF} = \frac{i(1+i)^n}{(1+i)^n - 1}$
Supplementary Cost	20% of Capital cost of equipment
Capital cost (CAPEX)	$C_{CAPEX} = C_R \times \left(\frac{C_{Act}}{C_{Ref}}\right)^n \times \left(\frac{I_{Act}}{I_{Ref}}\right)$
Operating expenditures	
Compression power cost	$= electricity\ cost \left(\frac{\$}{kW.yr}\right) \times compression\ power(kW)$
Cooling utility cost	$= cost\ of\ cooling\ media \left(\frac{\$}{kW.yr}\right) \times coolers\ nergy\ (kW)$
Labor cost	0.3% of capital cost
Maintenance cost	2% of capital cost
Other cost	1% of capital cost
Total cost	
Annualized cost, AC ($/y)	$AC = \left(\frac{CAPEX}{CRF}\right) + OPEX$
Unit production cost of LH_2, UPC ($/kg)	$UPC_{LH2} = \left(\frac{AC}{Capcity(kg/year)}\right)$

high heat transfer rate is a main process constraint. In this regard, the cost of cryogenic exchangers (plate fin type) are calculated through cost relations provided in ref [39] by considering the aluminum as material of construction. Cost of each equipment depends on its capacity which varies equipment to equipment and can be calculated through capital cost of equipment (C_{EC}) relation. Capital recovery factor (C_{RF}) was used to compute the annual capital expenses based on total equipment cost. In C_{RF} calculations, "i" denotes the discount rate while "n" represents the projected time of a new plant. Consequently, in CAPEX calculation, "C_R" represents the reference cost, "C" is capacity (actual/reference), and "n" is cost exponent, and "I" reflects the chemical engineering plant cost index (CEPCI). Moreover, annualized cost of proposed process is calculated to estimate the unit production cost (UPC) of LH_2.

Fig. 12 shows the annualized cost of proposed hydrogen liquefaction process where total cost is divided in to two sections, CAPEX and OPEX. It can be seen from Fig. 12 that the CAPEX is largely affected by the costs of compressors and heat exchangers. This is due to the reason of high energy required to liquefy hydrogen which ultimately raise the compressors cost while heat exchangers are made of expensive materials to ensure the high heat transfer and thus shares a major portion to elevate the overall cost of a process. As a result, compressors and heat exchangers shares are $>$ 81% in total CAPEX. Operating expenses are majorly due to compressor power and cooling utility for interstage cooling system. However, operating and maintenance cost has a huge share (65.8%) in OPEX, mainly due to large amount of equipment in each cooling cycle and their associated cost which requires maintenance and inspection for the balanced and proper functioning. Moreover, other cost is associated with OPEX which is 1% of total equipment cost. The annual capital cost is obtained through C_{RF}, hence the annualized cost (AC) of proposed process is obtained as \$1.89 $\times$ 10^6 /y based on 20 years of project life. In overall AC, CAPEX has $\sim$ 71.7% contribution however, this percentage of share varies from design to design and adopted methodology to liquefy H_2. In general, MR–based hydrogen liquefaction has high CAPEX and low OPEX [42].

Moreover, the projected cost analysis of proposed process was determined on the basis of enhanced capacity of liquified hydrogen as shown in Fig. 13. Since H_2–liquefaction is an energy and cost intensive process, a small-scale process is considered to be less attractive in development of H_2 economy. In this aspect, Linde [42] has demonstrated the scale up of H_2 liquefaction process and revealed that the expected unit production cost (UPC) will significantly reduce as the capacity factor is increased. Based on current process design, it can be seen from Fig. 13 that the capacity has major impact on specific cost of H_2 liquefaction. As the capacity enhanced from small to medium scale, the UPC significantly reduced especially, when capacity factor is enhanced from 0.1 to 1 TPD. As stated by Cardella et al. [12], the expected UPC of large scale liquefiers can be operated with $\leq$ \$1/kg of LH_2. In this regard, the proposed process demonstrates the similar trend of UPC (\$10.37 to 0.52) when capacity factor is increased from 0.5 to 50 TPD.

5. Conclusions

The precooling cycle is the most energy–intensive section of the H_2 liquefaction process as huge temperature drop (−159.4 °C) through a

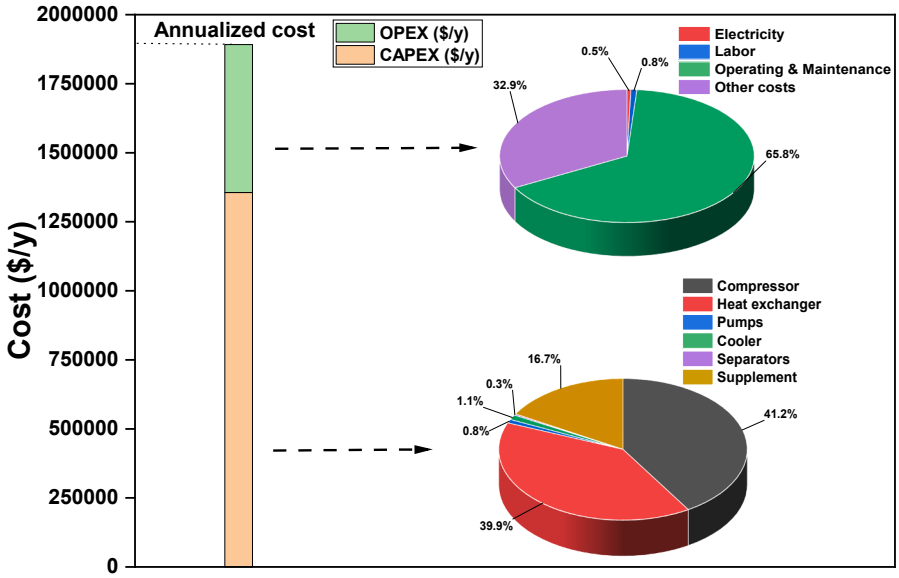


Fig. 12. CAPEX, OPEX, and annualized cost of proposed process.

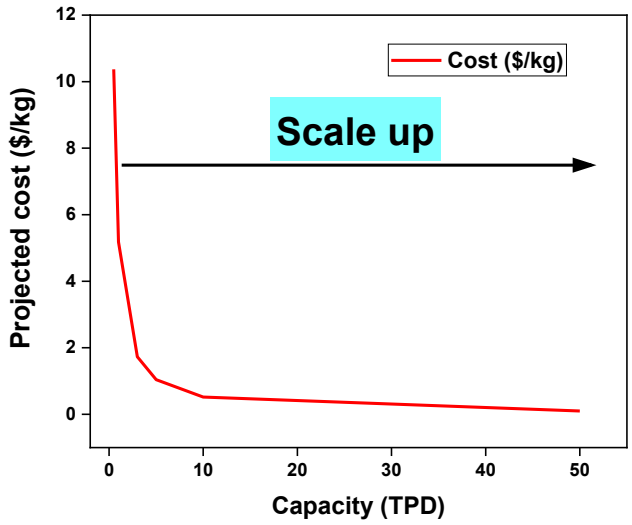


Fig. 13. Projected unit production cost of proposed process across enhanced capacity.

single refrigeration cycle is achieved in LH_2 process. Consequently, composite curve analysis depicted an energy saving opportunity with the unique selection of mixed refrigerants based on existing LH_2 processes. Therefore, considering the wide range of H_2 liquefaction temperature, precooling cycle was split into two cycles to achieve the similar goal with high energy efficiency and less exergy destruction. Process improvement was achieved by adding an additional precooling cycle–I based on an environmentally friendly high-boiling refrigerant, HFO-1234yf, with other mixed refrigerants. As a results, the peak of the approach temperature was significantly decreased based on composite curve analysis and thus the overall energy and exergy destruction was largely reduced throughout the system. Following outcomes were drawn from process enhancement of LH_2 process;

- Energy consumption of precooling cycle was reduced to 2.83 kWh that demonstrates the 51% and 32.6% less energy consumption as compared to base case–I and base case–II, respectively.
- The proposed process consumed 4.55 kWh/kgLH_2 of specific energy, which is 55.2% and 29.5% less than that of the base case–I and base case–II, respectively.
- Exergy destruction of proposed process was reduced from 6.13 to 3.17 kWh/kg of LH_2. The exergy efficiency of the proposed process increased from 47% to 67%.
- The reactor was added to improve the final conversion of para–H_2, ~99.5%, compared to the base case–II process with a final para concentration of ~ 95%.
- Economic evaluation resulted as the annual cost of proposed process is $\$1.89 \times 10^6$ /y while the estimated cost of unit production of LH_2 was \$5.18/kg with the capacity of 1TPD.

High energy efficiency is an attractive factor, but the proposed model still needs enhancement and analysis to evaluate its practical implementation on large scale. Advanced exergy and safety analysis can be the future approaches to locate the irreversibilities and sensitivity of the proposed model. Similarly, life cycle assessment can play a vital role to estimate the overall emissions to make it viable from theoretical stage to practical stage.

CRediT authorship contribution statement

Hyunhee Lee: Writing – original draft, Conceptualization, Methodology, Investigation, Data curation. **Junaid Haider:** Data curation, Formal analysis, Validation, Writing – original draft, Conceptualization, Methodology, Investigation. **Muhammad Abdul Qyyum:** Validation, Methodology, Conceptualization, Data curation, Investigation. **Changgwon Choe:** Formal analysis, Validation. **Hankwon Lim:** Conceptualization, Writing – review & editing, Supervision, Project administration.

Declaration of Competing Interest

The authors declare that they have no known competing financial interests or personal relationships that could have appeared to influence the work reported in this paper.

Acknowledgement

This work was supported by the 2022 Research Fund (1.220038.01) of UNIST (Ulsan National Institute of Science and Technology).

Appendix A. Supplementary data

Supplementary data to this article can be found online at https://doi.org/10.1016/j.fuel.2022.123964.

References

[1] Sher F, Al-Shara NK, Iqbal SZ, Jahan Z, Chen GZ. Enhancing hydrogen production from steam electrolysis in molten hydroxides via selection of non-precious metal electrodes. Int J Hydrogen Energy 2020;45:28260–71. https://doi.org/10.1016/J.IJHYDENE.2020.07.183.
[2] Lee B, Choe C, Kim H, Kim A, Shin YU, Haider J, et al. Economic parity analysis of green methanol synthesis using water electrolysis based on renewable energy. ACS Sustain Chem Eng 2021;9:15807–18. https://doi.org/10.1021/ACSSUSCHEMENG.1C05152/SUPPL_FILE/SC1C05152_SI_001.PDF.
[3] Al-Shara NK, Sher F, Yaqoob A, Chen GZ. Electrochemical investigation of novel reference electrode Ni/Ni(OH)₂ in comparison with silver and platinum inert quasi-reference electrodes for electrolysis in eutectic molten hydroxide. Int J Hydrogen Energy 2019;44:27224–36. https://doi.org/10.1016/J.IJHYDENE.2019.08.248.
[4] Al-Shara NK, Sher F, Iqbal SZ, Curnick O, Chen GZ. Design and optimization of electrochemical cell potential for hydrogen gas production. J Energy Chem 2021;52:421–7. https://doi.org/10.1016/J.JECHEM.2020.04.026.
[5] International Energy Agency (IEA). The Future of Hydrogen - Seizing today's opportunities. 2019. doi:10.1787/1e0514c4-en.
[6] Wolf J. Liquid hydrogen technology for vehicles. In: Vielstich W, Gasteiger HA, Lamm A, Yokokawa H, editors. Handb. Fuel Cells. John Wiley & Sons, Ltd; 2010. https://doi.org/10.1002/9780470974001.f302008.
[7] Cardella U, Decker L, Klein H. Roadmap to economically viable hydrogen liquefaction. Int J Hydrogen Energy 2017;42:13329–38. https://doi.org/10.1016/J.IJHYDENE.2017.01.068.
[8] Stolten D, Scherer V. Transition to Renewable Energy Systems. 2013. doi:10.1002/9783527673872.
[9] Stolzenburg K, Berstad D, Decker L, Elliott A, Haberstroh C, Hatto C, et al. Efficient Liquefaction of Hydrogen: Results of the IDEALHY Project 2013:7–9.
[10] Aasadnia M, Mehrpooya M. Large-scale liquid hydrogen production methods and approaches: a review. Appl Energy 2018;212:57–83. https://doi.org/10.1016/j.apenergy.2017.12.033.
[11] Stetson NT, McWhorter S, Ahn CC. Introduction to hydrogen storage. Compend Hydrog Energy, Woodhead Publishing 2016:3–25. https://doi.org/10.1016/b978-1-78242-362-1.00001-8.
[12] Cardella U, Decker L, Sundberg J, Klein H. Process optimization for large-scale hydrogen liquefaction. Int J Hydrogen Energy 2017;42:12339–54. https://doi.org/10.1016/J.IJHYDENE.2017.03.167.
[13] Krasae-In S, Bredesen AM, Stang JH, Neksa P. Simulation and experiment of a hydrogen liquefaction test rig using a multi-component refrigerant refrigeration system. Int J Hydrogen Energy 2011;36:907–19. https://doi.org/10.1016/J.IJHYDENE.2010.09.005.
[14] Krasae-In S, Stang JH, Neksa P. Simulation on a proposed large-scale liquid hydrogen plant using a multi-component refrigerant refrigeration system. Int J Hydrogen Energy 2010;35:12531–44. https://doi.org/10.1016/J.IJHYDENE.2010.08.062.
[15] Sadaghiani MS, Mehrpooya M, Ansarinasab H. Process development and exergy cost sensitivity analysis of a novel hydrogen liquefaction process. Int J Hydrogen Energy 2017;42:29797–819. https://doi.org/10.1016/J.IJHYDENE.2017.10.124.
[16] Sadaghiani MS, Mehrpooya M. Introducing and energy analysis of a novel cryogenic hydrogen liquefaction process configuration. Int J Hydrogen Energy 2017;42:6033–50. https://doi.org/10.1016/J.IJHYDENE.2017.01.136.
[17] Qyyum MA, Riaz A, Naquash A, Haider J, Qadeer K, Nawaz A, et al. 100% saturated liquid hydrogen production: Mixed-refrigerant cascaded process with two-stage ortho-to-para hydrogen conversion. Energy Convers Manag 2021;246:114659. https://doi.org/10.1016/J.ENCONMAN.2021.114659.

[18] Naquash A, Qyyum MA, Min S, Lee S, Lee M. Carbon-dioxide-precooled hydrogen liquefaction process: an innovative approach for performance enhancement–energy, exergy, and economic perspectives. Energy Convers Manag 2022;251:114947. https://doi.org/10.1016/J.ENCONMAN.2021.114947.
[19] Zhang S, Liu G. Design and performance analysis of a hydrogen liquefaction process. Clean Technol Environ Policy 2021;2021(1):1–15. https://doi.org/10.1007/S10098-021-02078-Z.
[20] Berstad DO, Stang JH, Nekså P. Comparison criteria for large-scale hydrogen liquefaction processes. Int J Hydrogen Energy 2009;34:1560–8. https://doi.org/10.1016/J.IJHYDENE.2008.11.058.
[21] Qyyum MA, Lee M. Hydrofluoroolefin-based novel mixed refrigerant for energy efficient and ecological LNG production. Energy 2018;157:483–92. https://doi.org/10.1016/J.ENERGY.2018.05.173.
[22] Zilio C, Brown JS, Schiochet G, Cavallini A. The refrigerant R1234yf in air conditioning systems. Energy 2011;36:6110–20. https://doi.org/10.1016/j.energy.2011.08.002.
[23] The Linde Group. Refrigerants environmental data: Ozone depletion and global warming potential. n.d.
[24] journal PJSBP-A, 2009 undefined. HFOs: new, low global warming potential refrigerants. SearchProquestCom n.d.
[25] Peng D, Robinson DB. A new equation of state. Nature 1929;123:507.
[26] Sherif SA, Goswami DY, Stefanakos EK, Steinfeld A. Handbook of hydrogen energy. Taylor & Francis; 2014.
[27] Hartl M, Gillis RC, Daemen L, Olds DP, Page K, Carlson S, et al. Hydrogen adsorption on two catalysts for the ortho- to parahydrogen conversion: Cr-doped silica and ferric oxide gel. Phys Chem Chem Phys 2016;18(26):17281–93.
[28] Woolley HW, Scott RB, Brickwedde FG. Compilation of Thermal Properties of Hydrogen in Its Various Isotopic and Ortho-Para Modifications n.d.
[29] Harkness RW, Deming WE. The equilibrium of para and ortho hydrogen. J Am Chem Soc 1932;54:2850–2. https://doi.org/10.1021/ja01346a503.
[30] Scott RB (Russell B, Denton WH, Nicholls CM. Technology and uses of liquid hydrogen n.d.:415.
[31] Asadnia M, Mehrpooya M. A novel hydrogen liquefaction process configuration with combined mixed refrigerant systems. Int J Hydrogen Energy 2017;42:15564–85. https://doi.org/10.1016/j.ijhydene.2017.04.260.
[32] Krasae-in S, Stang JH, Neksa P. Development of large-scale hydrogen liquefaction processes from 1898 to 2009. Int J Hydrogen Energy 2010;35:4524–33. https://doi.org/10.1016/j.ijhydene.2010.02.109.
[33] Design KW-CER and, 2009 undefined. Complexity of chemical products, plants, processes and control systems. Elsevier n.d.
[34] Comments on the paper by Baldur Eliasson and Ulf... - Google Scholar n.d. https://scholar.google.com/scholar?q=Comments on the paper by Baldur Eliasson and Ulf Bossel The future of the hydrogen economy: bright or bleak (accessed February 9, 2022).
[35] Bracha M, Lorenz G, Patzelt A, Wanner M. Large-scale hydrogen liquefaction in Germany. Int J Hydrogen Energy 1994;19:53–9. https://doi.org/10.1016/0360-3199(94)90177-5.
[36] Kaeltetechnik HQ-KL, 2002 undefined. The key role of cryogenics in the future hydrogen energy economy; Die Schluesselrolle der Kryotechnik in der Wasserstoff-Energiewirtschaft. OstiGov n.d.
[37] Berstad DO, Stang JH, Nekså P. Large-scale hydrogen liquefier utilising mixed-refrigerant pre-cooling. Int J Hydrogen Energy 2010;35:4512–23. https://doi.org/10.1016/J.IJHYDENE.2010.02.001.
[38] Naquash A, Haider J, Qyyum MA, Islam M, Min S, Lee S, et al. Hydrogen enrichment by CO2 anti-sublimation integrated with triple mixed refrigerant-based liquid hydrogen production process. J Clean Prod 2022;341:130745.
[39] Turton R, Bailie RC, Whiting WB, Analysis SJA. synthesis and design of chemical processes. Pearson Education; 2008.
[40] Ahmad F, Lau KK, Shariff AM, Murshid G. Process simulation and optimal design of membrane separation system for CO 2 capture from natural gas. Comput Chem Eng 2012;36:119–28. https://doi.org/10.1016/j.compchemeng.2011.08.002.
[41] Nordio M, Wassie SA, Van Sint AM, Pacheco Tanaka DA, Viviente Sole JL, Gallucci F. Techno-economic evaluation on a hybrid technology for low hydrogen concentration separation and purification from natural gas grid. Int J Hydrogen Energy 2021;46:23417–35. https://doi.org/10.1016/j.ijhydene.2020.05.009.
[42] Cardella U. Large-scale liquid hydrogen production and supply advancing H mobility and clean. Energy 2019.